Technical Sciences
Academy of Romania
www.jesi.astr.ro

Journal of Engineering Sciences and Innovation
Volume 7, Issue 3 / 2022, pp. 335 - 348
http://doi.org/10.56958/jesi.2022.7.3.335

C. Chemical Engineering, Materials Science and Engineering

Received ***3 June 2022*** *Accepted* ***14 September 2022***
Received in revised form ***18 August 2022***

New in-situ composite materials with aluminium alloy matrix (6063) and vanadium boride particles

PETRU MOLDOVAN, MIHAI BUȚU, CONSTANTIN-DOMENIC STĂNCEL*

Politehnica University of Bucharest, Splaiul Independentei nr. 313, Bucharest, Romania

Abstract. The exothermic reactions between AA 6063 alloy, AlV master alloy, and inorganic salt mixture (KBF_4) result in the fabrication of matrix alloy 6063 reinforced by in-situ obtained VB_2 particles via liquid metallurgy. The presence of VB_2 was revealed using optical microscopy and by the XRD patterns. The reinforcing particles act as a grain refiner at 1% concentration of VB_2. A set of compressive tests were taken to showcase the compressive stress-strain curves of the different samples at different concentrations of VB_2.

Keywords: MMCs, VB_2 particles, Compressive stress-strain curves

1. Introduction

Particle reinforced MMCs are appealing due to their low cost, isotropic characteristics, and ability to be manufactured utilizing monolithic material technology. Discontinuously reinforced MMCs have improved physical and mechanical properties that conventional engineering alloys cannot match [1], [2].
A wide variety of in-situ formed ceramic particulates (Al_2O_3, TiB_2, ZrB_2 and AlN) has been established to produce Aluminium-Matrix-Composites [3]. In-situ production of Aluminium Matrix Composites consists of aluminothermic reaction between Aluminium (or Aluminium alloy) and salts (direct melt synthesis). The major advantages over ex-situ composites include excellent bond and improved thermodynamic compatibility between particles and matrix.

*Correspondence address: stancel.constantin@yahoo.com

The present study is an attempt to explore the processing of in situ new Aluminium Matrix Composites using an AA6063 master alloy and VB_2 as reinforcement materials.

2. Elaboration of AA 6063/VB_2 composites

The in situ AA6063/VB_2 composite is being fabricated by exothermic salt-metal reaction, using AlV10 master alloy, KBF_4 and molten AA6063 alloy.
In order to obtain tensile test bars and samples for XRD analysis, the composite melts were poured into the pre-heated rod-shaped mould with ϕ = 12 mm and h = 90 mm at different VB_2 concentrations (1%, 2%, 3%, 4%, 5% and 10%). [4]
HSC Chemistry was used to test the Gibbs free energy formations for aluminium and vanadium borides at temperatures ranging from 680°C to 860°C. (Table 1). The stability curves of the various possible reactions are shown in Figure 1. Through thermodynamic analysis of the reactions occurring in the melt, we found that the reaction (1) was the most likely reaction to occur during the composite development. The VB_2 diboride phase is predicted to be more stable in the given conditions than other phases, VB, V_3B_4, and V_5B_6.

$$6KBF_4 + 3V\ (AlV10) + 6Al\ (AA6063) = 3VB_2 + 2K_3AlF_6 + 4AlF_3 \quad (1)\ [4]$$
$$2KBF_4 + V + 2Al = VB_2 + 2KF + 2AlF_3 \quad (2)\ [4]$$
$$3Al + 1.5V + Na_3AlF_6 + 3KBF_4 = 1.5VB_2 + K_3AlF_6 + 3AlF_3 + 3NaF \quad (3)\ [4]$$

Table 1. The Gibbs free energy formations for the reactions

T	deltaG (1)	deltaG (2)	deltaG (3)
C	kJ	kJ	kJ
680	-884.137	-503.194	-781.753
700	-879.188	-499.538	-776.096
720	-874.233	-495.871	-770.430
740	-869.272	-492.195	-764.757
760	-864.306	-488.511	-759.078
780	-859.337	-484.820	-753.392
800	-854.363	-481.121	-747.703
820	-849.388	-477.417	-742.009
840	-844.411	-473.706	-736.312
860	-839.433	-470.141	-730.614

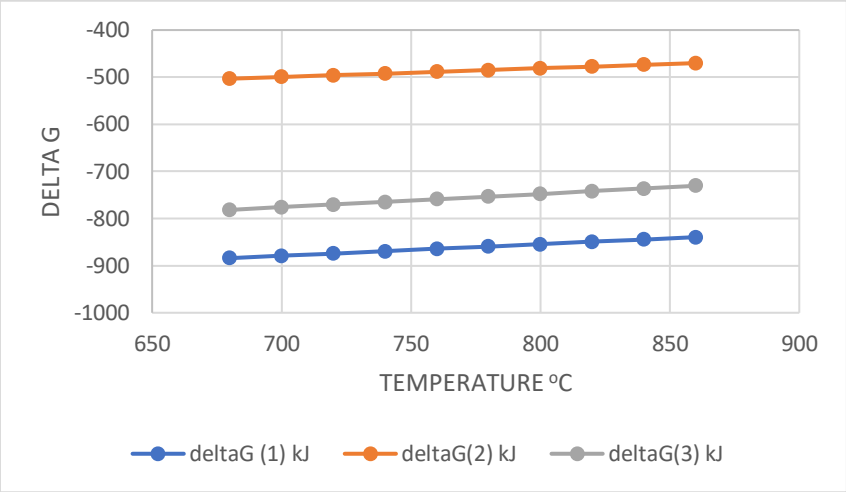

Figure 1. The Ellingham temperature diagram for the reactions

3. Microstructure of the composites

The obtained VB_2 particles crystallizes in the hexagonal system with structure type AlB_2 and calculated density ρ = 5.00 g/cm^3 [5].
An optical microscopy analysis of the material in an intermediate state was performed to determine the mechanism of the aforementioned reactions.
At 1% VB_2, the reinforcing particles operate as a grain refiner, and the microstructures are not visible in optical micrographs or diffractograms.
Figure 2 shows an optical micrograph of a typical boride phase microstructure (a). The optical micrograph in Figure 2 shows a ring of mid-grey borides surrounding the typical microstructure of boride phases (a).
Samples with over 3% VB_2 contained undissolved black particles (AlB_{12}), which provided boron for the completion of the reaction with V during boron treatment.

VB_2 1% x500

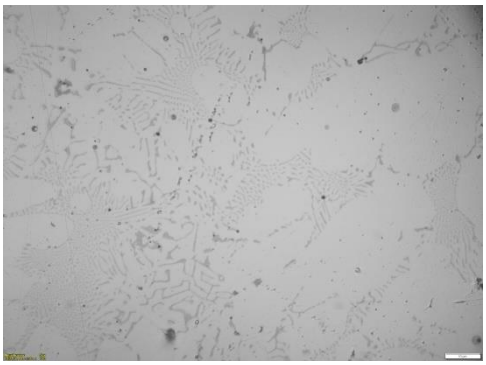

VB_2 1% x1000

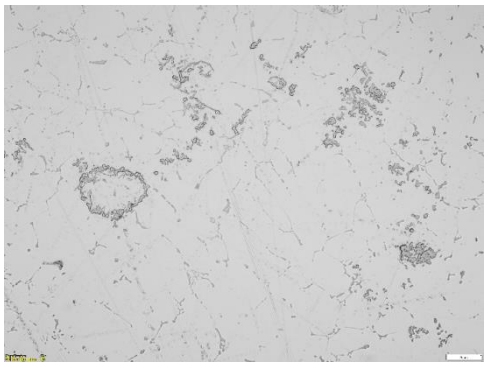

VB_2 2% x500

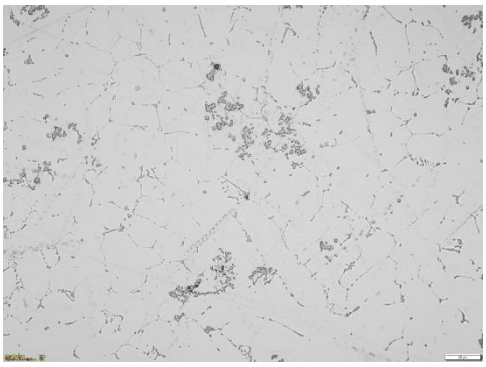

VB_2 2% x500

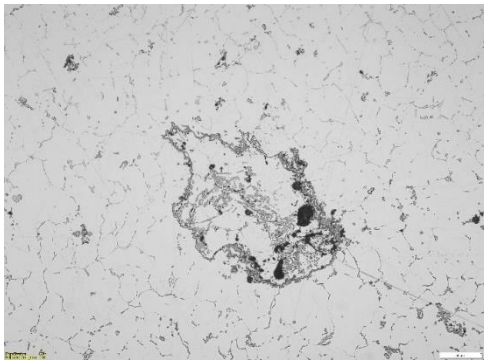

VB_2 3% x200

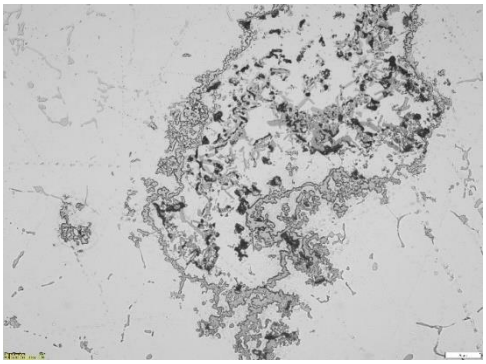

VB_2 3% x500

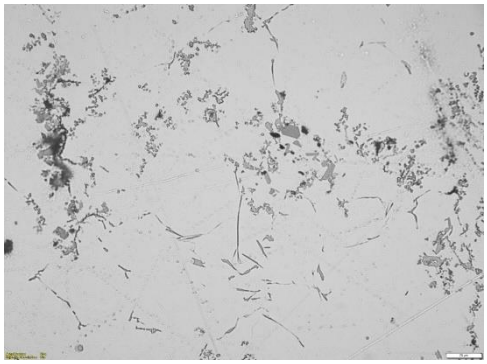

VB_2 4% x500

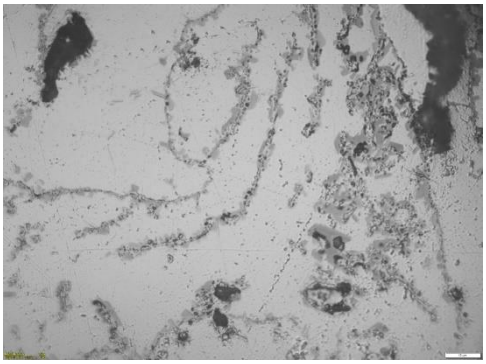

VB_2 4% x1000

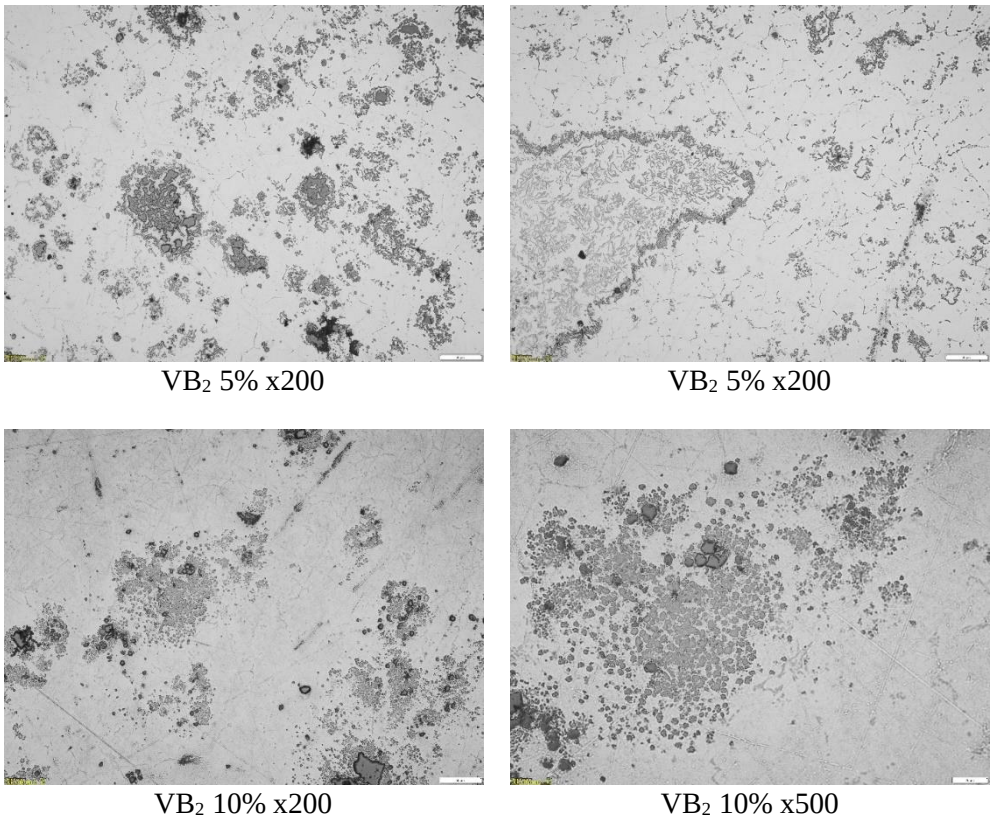

VB_2 5% x200 VB_2 5% x200

VB_2 10% x200 VB_2 10% x500

Fig. 2. Optical micrograph of the samples with different concentrations of VB_2

The agglomeration of VB_2 particles occurs when the concentration of particles increases.

4. Diffractometric analysis

The samples were diffractometrically analysed in order to identify the VB_2 particles. Figures 3–15 show the diffractometric analysis results for the analysed samples (1,2,3,4,5,10% VB_2).

The data processing was done with the help of the DIFFRAC.EVA Release 2019 Ver. 5.1 program of the DIFFRAC.SUITE.EVA software package and the ICDD PDF4 + 2020 database.

4.1 Sample 1

4.1.1. Primary data:

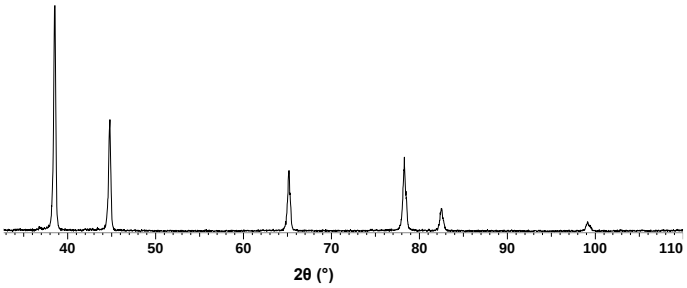

Fig. 3. Diffractogram Sample 1 (primary data).

4.1.2. Phase analysis

The phase analysis was performed using the DIFFRAC.EVA release 2019 software and the ICDD PDF4 + 2020 database**.**

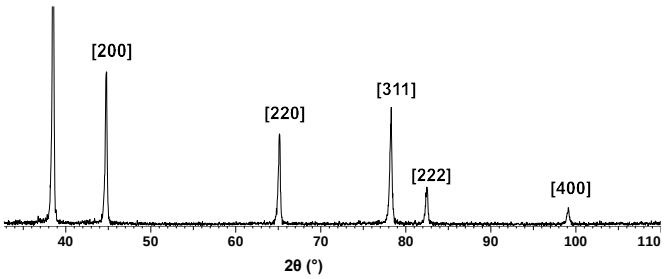

Compound Name	Reference PDF	Chemical Formula	Crystallization System	Spatial Group
Ss type A1	04-017-1423	Ss Type A1- $Al_{1-x}M_x$ (prototype Cu)	Cubic (Cube with centered faces)	Fm-3m (225)

Fig. 4. Graphic presentation of the qualitative phase analysis using XRD for Sample 1

4.2 Sample 2

4.2.1. Primary data:

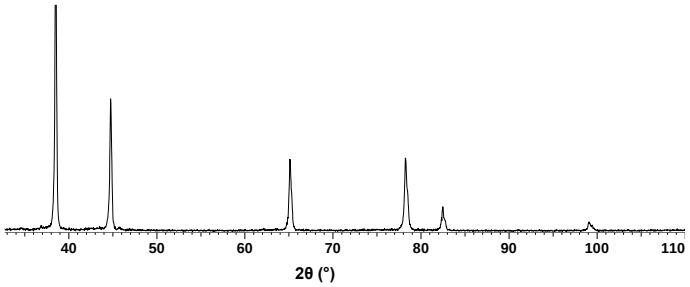

Fig. 5. Diffractogram Sample 2 (primary data)

4.1.2. Phase analysis:

The phase analysis was performed using the DIFFRAC.EVA release 2019 software and the ICDD PDF4 + 2020 database**.**

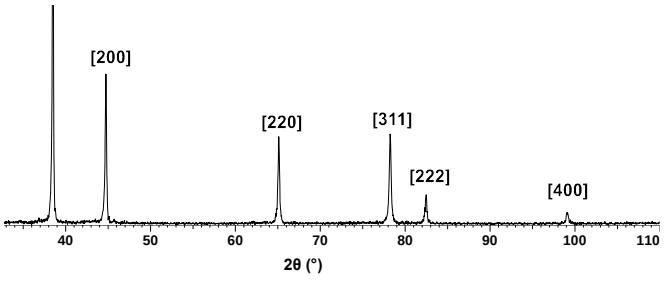

Compound Name	Reference PDF	Chemical Formula	Crystallization System	Spatial Group
Ss type A1	04-017-1423	Ss Type A1- $Al_{1-x}M_x$ (prototype Cu)	Cubic (Cube with centered faces)	Fm-3m (225)

Fig. 6. Graphic presentation of the qualitative phase analysis using DRX for Sample 2

4.3. Sample 3

4.3.1. Primary data:

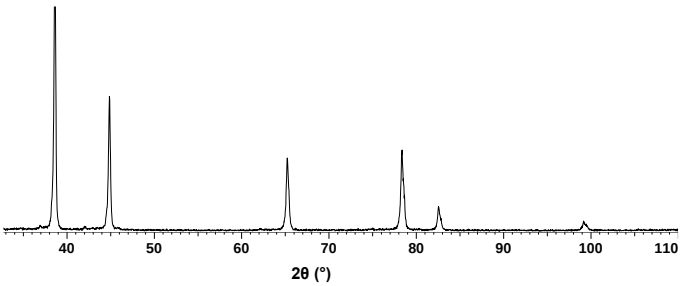

Fig. 7. Diffractogram Sample 3 (primary data).

4.3.2. Phase analysis:

The phase analysis was performed using the DIFFRAC.EVA release 2019 software and the ICDD PDF4 + 2020 database**.**

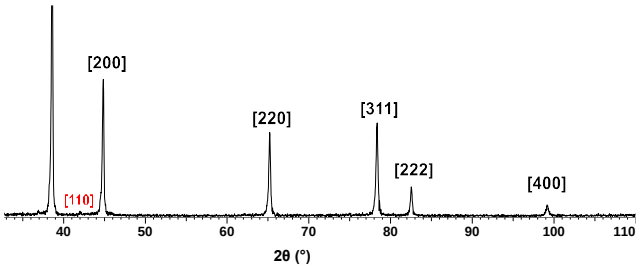

Compound Name	Reference PDF	Chemical Formula	Crystallization System	Spatial Group
Ss type A1	04-017-1423	Ss Type A1- $Al_{1-x}M_x$ (prototype Cu)	Cubic (Cube with centered faces)	Fm-3m (225)
AlV_2	01-077-6859	AlV_2	Cubic (Cube with centered volume)	Im-3m (229)

Fig. 8. Graphic presentation of the qualitative phase analysis using XRD for Sample 3

4.4 Sample 4

4.4.1. Primary data:

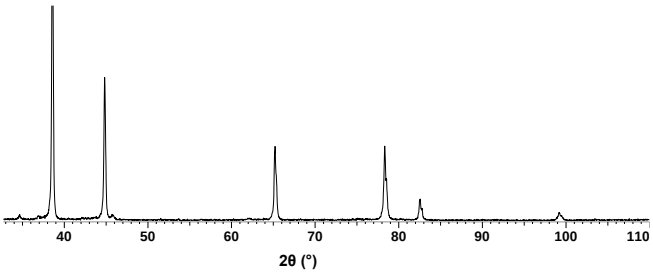

Fig. 9. Diffractogram Sample 4 (primary data).

4.4.2. Phase analysis:

The phase analysis was performed using the DIFFRAC.EVA release 2019 software and the ICDD PDF4 + 2020 database**.**

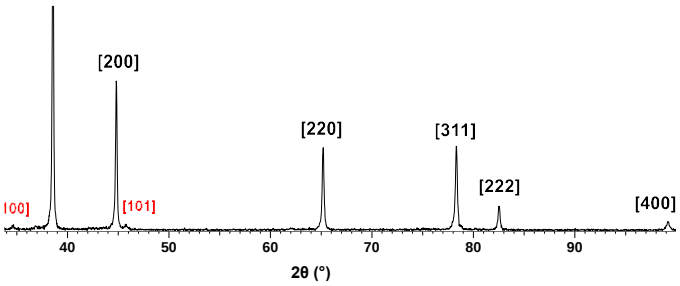

Compound Name	Reference PDF	Chemical Formula	Crystallization System	Spatial Group
Ss type A1	04-017-1423	Ss Type A1- $Al_{1-x}M_x$ (prototype Cu)	Cubic (Cube with centered faces)	Fm-3m (225)
VB_2	00-038-1463	VB_2	Hexagonal	P6/mmm (191)

Fig. 10. Graphic presentation of the qualitative phase analysis using XRD for Sample 4

4.5 Sample 5

4.5.1. Primary data:

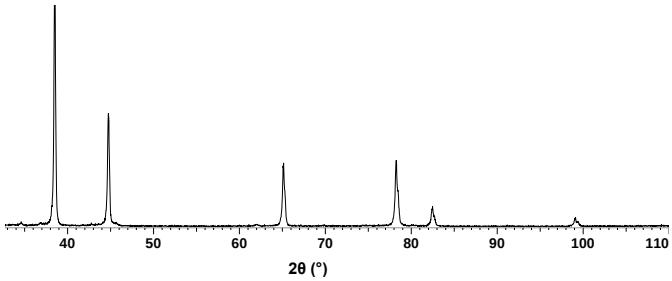

Fig. 11. Diffractogram Sample 5 (primary data).

4.5.2. Phase analysis:

The phase analysis was performed using the DIFFRAC.EVA release 2019 software and the ICDD PDF4 + 2020 database**.**

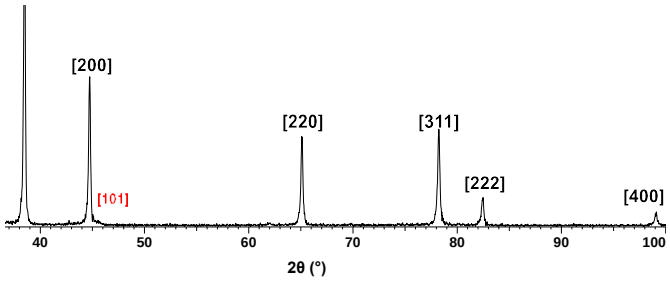

Compound Name	Reference PDF	Chemical Formula	Crystallization System	Spatial Group
Ss type A1	04-017-1423	Ss Type A1- $Al_{1-x}M_x$ (prototype Cu)	Cubic (Cube with centered faces)	Fm-3m (225)
VB_2	00-038-1463	VB_2	Hexagonal	P6/mmm (191)

Fig. 12 Graphic presentation of the qualitative phase analysis using XRD for Sample 5

4.6. Sample 6

4.6.1. Primary data:

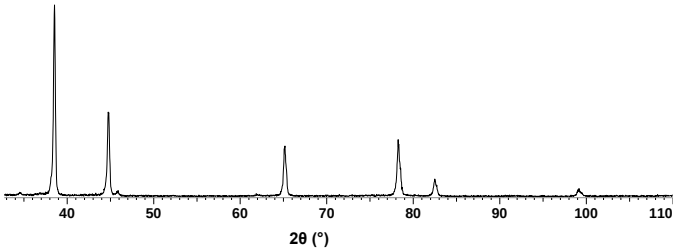

Fig. 13. Diffractogram Sample 6 (primary data)

4.6.2. Phase analysis:

The phase analysis was performed using the DIFFRAC.EVA release 2019 software and the ICDD PDF4 + 2020 database**.**

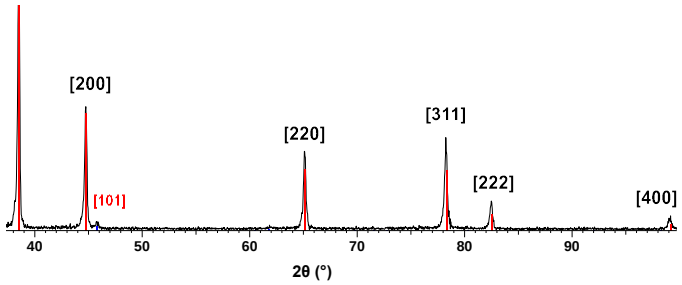

Compound Name	Reference PDF	Chemical Formula	Crystallization System	Spatial Group
Ss type A1	04-017-1423	Ss Type A1- $Al_{1-x}M_x$ (prototype Cu)	Cubic (Cube with centered faces)	Fm-3m (225)
VB_2	00-038-1463	VB_2	Hexagonal	P6/mmm (191)

Fig. 14. Graphic presentation of the qualitative phase analysis by DRX for Sample 6

In processing the collected experimental data, the following aspects were considered:
The fund (regarded as information contained in the data collected) was removed from the qualitative phase analysis.
The Kα2 component has been removed.
X-ray diffraction analysis of the six samples prepared in the form of chips revealed the following:
Existence in all 6 samples of a main structure of cubic symmetry: Cube with centered faces - type A1) which can be associated with a solid solution of Aluminium with Si, Mg.
At low concentrations of up to 2% no formation of new crystalline structures is observed. At a percentage of 3% there is the appearance of a line characteristic of plane 110 of the cubic structure with centered volume, but which cannot be attributed to a certain compound, because other diffraction maxima are not visible. This is due to the low concentration of this phase, so that the diffraction maxima are below the detection limit. According to the literature, this structure can be attributed to the compound AlV_2.
Once the concentration increases from 4 to 6%, the formation of a hexagonal compound of type VB_2 is observed. Its characteristic maxima can be easily observed on the diffractogram.

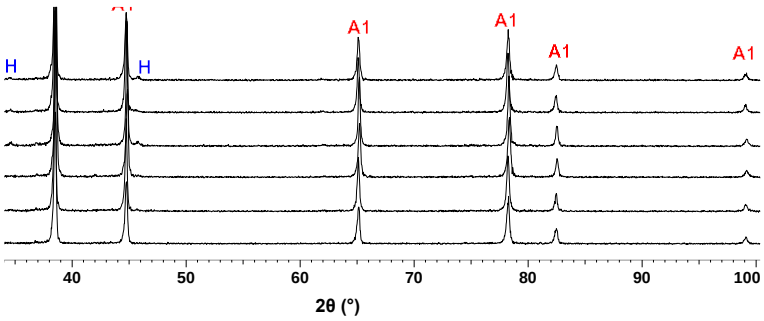

Fig. 15. Graphical representation of the diffractograms of the six samples

5. Compressive studies of 6063/VB_2 composites

The true stress-strain curves of the composites under compression loading at room temperature are shown in Figure 16.

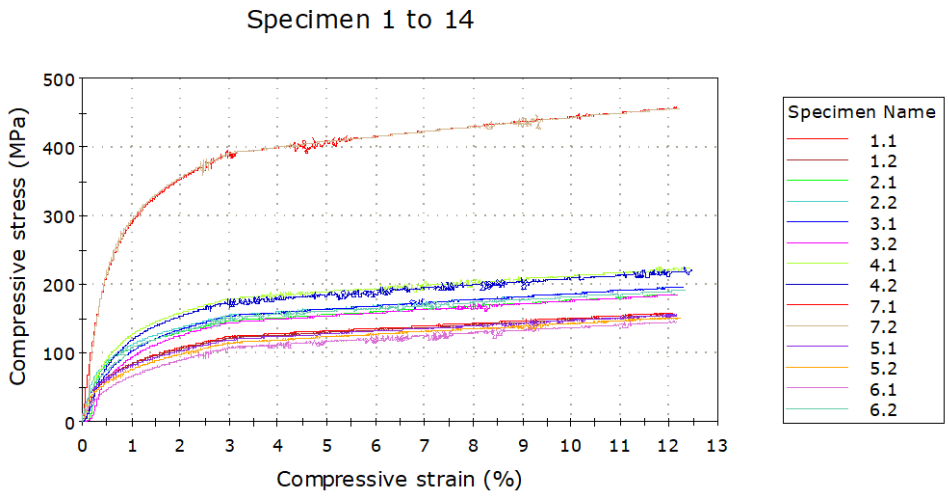

Fig. 16. Compressive stress-strain curves of AA6063 %VB_2 composites

An improvement in the strength by adding in-situ VB_2 particles are observed [6]. The samples used were analysed at a test speed 0,5 mm/min.

6. Conclusions

A new AA6063/VB_2 in situ composites containing different volume fraction can be successfully developed by in-situ reaction of molten aluminium alloy with KBF4 and AlV10 master alloy.

Microstructural examinations show the distribution of VB_2 particles with different concentrations.

The XRD spectrum of composites confirms the formation of a hexagonal compound of type VB_2.

The true stress-strain curves of the composites under compression loading are examined.

Improved stirring of the melt will aid in the redistribution of impurities. This increases the concentration gradient as well as the mass transfer of transition metal impurities and boron.

Treatment with melt degassing fluxes and cryolite aids in the redistribution of transition metal boride solid particles around AlB_{12} / AlB_2 particles.

References

[1] Moldovan P., *Metal matrix composites*, Bucharest, PRINTECH, 2008.

[2] Moldovan P., Buțu M., *Thermodynamics of in situ formation of TiB2 particulates in complex aluminium alloys for aeronautics*, Journal of Engineering Sciences and Innovation, **4**, 3, p. 285-300, 2019.

[3] Wang Y., Wang H., Xiu K., Wang H. and Jiang Q., *Fabrication of TiB2 particulate reinforced*

magnesium matrix composites by two-step processing method, Materials Letters, **60**, 12, p. 1533-1537, 2006.

[4] Buțu M., Ogica C., Marcu D. F., Stăncel C. D., Niculescu F.and Drăguț V. D., *Obtaining of AA6063/VB2 composites produced by aluminothermic reaction*, U.P.B. Sci. Bull., Series B, **83**, 2, 2021, p. 209 - 220.

[5] Buțu M., Moldovan P., Roșu L., Stăncel C.-D., Ogica C., Buțu L. and Marinescu M., *Research studies on obtaining metastable intermetallic structures in 6xxx/borides composites*, UPB Scientific Bulletin, Series B, 82, 2, 2020, p. 185-197.

[6] Matli P. R., Shakoor R. A. and Mohamed A. M. A., *Development of Metal Matrix Composites Using Microwave Sintering Techniqu*e, in *S*intering of Functional Materials, Chapter 2, INTECH, 2018, p. 23-43.